

Long-lived mesoscopic entanglement outside the Lamb-Dicke regime

M. J. McDonnell, J. P. Home, D. M. Lucas, G. Imreh, B. C. Keitch,

D. J. Szwer, N. R. Thomas, S. C. Webster, D. N. Stacey and A. M. Steane.

Clarendon Laboratory, Department of Physics, University of Oxford, Parks Road, Oxford OX1 3PU, UK

We create entangled states of the spin and motion of a single $^{40}\text{Ca}^+$ ion in a linear ion trap. The motional part consists of coherent states of large separation and long coherence time. The states are created by driving the motion using counterpropagating laser beams. We theoretically study and experimentally observe the behaviour outside the Lamb-Dicke regime, where the trajectory in phase space is modified and the coherent states become squeezed. We directly observe the modification of the return time of the trajectory, and infer the squeezing. The mesoscopic entanglement is observed up to $\Delta\alpha = 5.1$ with coherence time $170\ \mu\text{s}$ and mean phonon excitation $\bar{n} = 16$.

A two-state system interacting with a quantum harmonic oscillator has for a long time played a fundamental role in quantum optics [1], and more recently has attracted interest in the context of mesoscopic quantum physics, micromechanical oscillators [2, 3], and quantum information [4, 5]. The states of motion of a quantum oscillator which most closely resemble classical states of motion are the Glauber coherent states [1]. It has been pointed out that a superposition of such states, with a large difference between their coherent state parameters α , is a state of affairs comparable to the Schrödinger Cat thought-experiment [1, 6]. This permits an investigation of mesoscopic quantum physics using this system. The conditions of the thought-experiment are most closely matched when the superposition involves an entanglement between the large system (the oscillator) and a smaller (e.g. two-state) system, viz:

$$|\psi\rangle = \frac{1}{\sqrt{2}} (|\alpha_{\uparrow}\rangle |\uparrow\rangle + e^{i\varphi} |\alpha_{\downarrow}\rangle |\downarrow\rangle) \quad (1)$$

where $\Delta\alpha^2 = |\alpha_{\uparrow} - \alpha_{\downarrow}|^2$ is large, $|\uparrow\rangle, |\downarrow\rangle$ are the states of the two-state system, and the interference phase φ must be stable and under control in the experiment (as must the values of $\alpha_{\uparrow, \downarrow}$, including their relative phase).

The coherent states are mesoscopic in that their energy is $\bar{n} = |\alpha|^2 \gg 1$ units of the fundamental excitation energy (the energy gap between the ground and first excited states) and the separation x_s of the motional wavepackets is greater than their individual size x_0 by the ratio $x_s/x_0 = 2\Delta\alpha \gg 1$. The size of the Hilbert space required to express the motional state is approximately $\log_2 \bar{n}$ qubits, and in the case of a state such as (1) there is entanglement with another degree of freedom. The phase coherence time, T_2 , is sensitive to the separation [7]. These measures are summarized by the list $\{\bar{n}, \Delta\alpha, x_s, T_2\}$.

States of the type (1) have been realized in the internal state and motion of single trapped ions [8, 9, 10], and in an atom interacting with a cavity-field [11, 12]. For experiments where the coherence of the two parts of the state was observed [13], the reported parameter values were $\{\bar{n}, \Delta\alpha, x_s, T_2\} = \{8.8, 2.97, 42\text{nm}, O(10\ \mu\text{s})\}$ [8];

$\{12, 5.2, 73\text{nm}, 6\ \mu\text{s}\}$ [9]; $\{1, 2, 14\text{nm}, \sim 0.5\text{ms}\}$ [10]; $\{9.5, 1.8, \text{---}, 90\ \mu\text{s}\}$ [11].

We present experiments in which the cat state is realized with large values of both the size and the coherence time together, and we describe and demonstrate a qualitatively new behaviour which appears outside the Lamb-Dicke regime (LDR). We have generated cat states of the spin and motion of a single trapped $^{40}\text{Ca}^+$ ion with $\{\bar{n}, \Delta\alpha, x_s, T_2\} = \{16, 5.1, 170\text{nm}, \simeq 170\ \mu\text{s}\}$, observing their coherence using an interference effect. The Hilbert space dimension is approximately 5 qubits. In our experiments the driving of the motion goes outside the LDR: that is, the force on the ion is not independent of its position, in contrast to previous work. This results in a dramatic modification of the trajectory in phase space, and also squeezing of the coherent state [14]. This means that we achieve cat states of the traditional type, and also infer production of states in which the entangled and subsequently interfering components are not standard coherent states, but squeezed states, with a squeezing parameter (ratio of principal axes of the Wigner function) $\simeq 3$.

Our system consists of a single spin-half particle in a harmonic potential, subject to a “walking wave” of light formed by counterpropagating laser beams in a standing wave configuration with a frequency difference applied between the two beams. The walking wave provides a spin-dependent force on the particle. The interaction Hamiltonian is $H_I = H_{\pi} + \sum_m V_m |m\rangle \langle m|$ where $m = \uparrow, \downarrow$,

$$V_m = \hbar\Omega \cos(k\hat{x} - \omega t + \phi_m) \quad (2)$$

and $H_{\pi} = \hbar\Delta_{\pi}(|\uparrow\rangle \langle \uparrow| - |\downarrow\rangle \langle \downarrow|)/2$. V_m is a light shift from far-off-resonant single-photon excitation; H_{π} is a light shift from off-resonant Raman excitation of spin-flip transitions. The latter has no effect on the motion, but causes the spin state to precess. k and ω are the wavevector along the x axis and the frequency of the walking wave respectively.

The position-dependence of V_m results in a spin-dependent force $f_m(x, t) = -dV_m/dx$. The classical equation of motion is $2M\omega_0 x_0 (d\alpha/dt) =$

$i \exp(i\omega_0 t) f_m(x, t)$ where $\alpha = \exp(i\omega_0 t)(x + ip/M\omega_0)/2x_0$, and x_0 is a length scale. M is the mass of the ion and ω_0 its natural oscillation frequency in the trap. If we take $x_0 = (\hbar/2M\omega_0)^{1/2}$ then α corresponds exactly to the coherent state parameter in the quantum treatment.

We consider motional states $|\alpha\rangle$ starting at or near $\alpha = 0$. For small $|\langle kx \rangle|$ we have the LDR, where the force $f_m(x, t) \simeq \hbar\Omega k \sin(\omega t - \phi_m)$ is independent of position. In this case an analytical solution of the time-dependent Schrödinger equation (TDSE) is possible [1, 15, 16]. The quantum state is merely displaced along a trajectory $\alpha(t)$ exactly matching the classical prediction. For $|\delta| \ll \omega_0$ where $\delta = \omega - \omega_0$, $\alpha(t)$ describes a circle of diameter $\eta\Omega/\delta$, where $\eta = kx_0$ is the Lamb-Dicke parameter. The motion around the circle is at a constant rate, completing a loop at integer multiples of $2\pi/\delta$. The quantum state picks up a phase proportional to the area of the loop, plus a contribution $\pm\Delta_\pi t/2$, and an oscillating phase from $\int V_m dt$. This oscillating phase scales as $1/\eta$; it is important when $\langle kx \rangle \ll 1$ but is small outside the LDR when $\langle kx \rangle \sim 1$ and we will ignore it hereafter.

Outside the LDR, the classical dynamics cannot be solved analytically. We have studied this by numerical analysis: a numerical integration of the classical equation of motion, and an approximate numerical solution of the TDSE. The latter included up to $n_{\max} = 100$ harmonic oscillator levels and terms in all orders of η for the carrier and first three motional sidebands in H_I .

The position dependence of the force causes the trajectory to be non-circular and the motional state is squeezed, that is, the wavepacket is narrowed in one direction in phase space and broadened in another. For modest values of $\langle kx \rangle$ we find that the squeezing is negligible and the quantum wavepacket simply follows the modified classical trajectory. For larger values the wavepacket is squeezed, and for larger values still, or longer times (e.g. after more than one loop in phase space) the wavepacket changes shape dramatically. Figure 1 shows an illustrative example. The departure from a circular trajectory and the squeezing are clearly seen. Note that $\alpha(\tau)$, where τ is the length of time that the force is applied, still returns to the origin, but at a time t_r earlier than the value $2\pi/\delta$ for a state which stays within the LDR.

We find $\alpha(\tau)$ begins to differ clearly from a circle when $\langle kx_{\max} \rangle = 2\eta|\alpha_{\max}| > 1$. Each loop is shaped like a tear-drop and t_r is reduced. Fortunately, there are two features of the motion which simplify the interpretation of our experiments. First, in the early stages, it is still within the LDR so the initial behaviour both in terms of amplitude and phase is accurately described by the simple analytical treatment outlined above. Second, when the amplitude of the motion drops for the first time back into the LDR the analytical treatment again gives a good

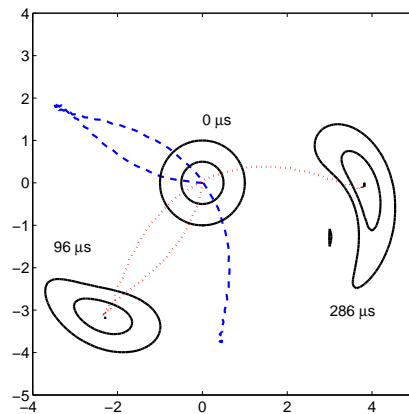


FIG. 1: (color online) Trajectories in phase space $\alpha(\tau)$ (dotted and dashed lines) and motional Wigner function (contour lines at 0,1,2 standard deviations) for the parameter values $\omega_0/2\pi = 536$ kHz, $\eta = 0.244$, $\Omega/2\pi = 93$ kHz, $\delta/2\pi = 3.4$ kHz and varying forcing time τ . The two trajectories are shown for the different spin states for $\Phi_w = 1.41$, up to the time $2\pi/\delta = 286 \mu\text{s}$. $\Phi_w = |\phi_\uparrow - \phi_\downarrow|$ is the phase angle between the forces on the two spin states. The return time is $t_r = 192 \mu\text{s}$. For clarity, the Wigner function is shown for just one of the trajectories at three example times, $\tau = 0, 96, 286 \mu\text{s}$. The squeezing is $\simeq 3$ at $t_r/2$. In the experiments, superpositions of motion along both members of such pairs of trajectories are created.

representation of the behaviour, if one takes into account the difference between the actual and LDR return times.

We experimentally investigated the behaviour using a single $^{40}\text{Ca}^+$ ion in a linear ion trap [17]. The two-state system is the spin-1/2 ground state of the ion, and the potential (2) is realized by the light shift when the ion is illuminated by a laser walking wave far (30 GHz) detuned from the $\lambda = 397$ nm $S_{1/2}$ - $P_{1/2}$ transition. A quantization axis is defined by a 1.4 Gauss magnetic field \mathbf{B} at 57° to the trap axis x . These axes are horizontal. A 60° pair of laser beams forms the walking wave along x , with difference wavevector $k = 2\pi/\lambda$. Their difference frequency ω is generated with 1 Hz precision by acousto-optic modulation. One beam is horizontally polarized, the other is close to linear at 69° to the vertical. The resulting light field has three components: a σ^+ polarized walking wave, a σ^- polarized walking wave, and a predominantly π polarized travelling wave. The transition in the ion is $J = \frac{1}{2} \rightarrow \frac{1}{2}$, so the σ^+ (σ^-) light interacts with $|\downarrow\rangle$ ($|\uparrow\rangle$), giving rise to V_\downarrow , (V_\uparrow) respectively.

The ion is first prepared in $|\downarrow\rangle|\bar{n}_0\rangle$ where $|\bar{n}_0\rangle$ is a thermal motional state close to the ground state with mean motional state occupation number \bar{n}_0 [18]. A sequence of laser pulses is then applied, and finally the spin state is measured by selective shelving followed by fluorescence detection, see [19]. This is repeated 500 times to accumulate statistics, then a parameter value is changed and the sequence repeated.

Initial experiments were carried out by Ramsey inter-

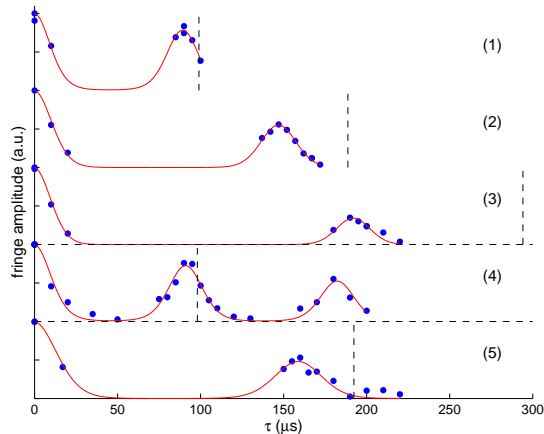


FIG. 2: Observed fringe amplitudes as a function of τ , normalized to the value at $\tau = 0$. Each point is obtained from a sin fit to a scan over ϕ . The lines are fitted curves using (4), with parameter values given in table 1. Dashed horizontal lines separate data sets taken at different trap frequencies. Dashed vertical lines are drawn at $\tau = 2\pi/\delta$.

ferometry, with the oscillating force pulse \mathcal{W} applied in the gap. The $\pi/2$ pulses were Raman transitions driven by the walking wave, with tunable relative azimuthal phase ϕ . The data reported here were obtained using a spin-echo sequence, to eliminate slow phase noise. The first $\pi/2$ pulse evolves the spin to $(|\uparrow\rangle + |\downarrow\rangle)/\sqrt{2}$. After the \mathcal{W} pulse, of duration τ , the system is (up to a global phase) in the state (1), with $\varphi = \Delta_\pi\tau$. In the LDR, $|\alpha_{\uparrow,\downarrow}\rangle$ are coherent states, and outside this limit they are squeezed or more general states, centred in phase space close to $\alpha_{\uparrow,\downarrow}$. The observed signal after the final pulse is

$$P(\uparrow) = \left(1 - \text{Re} \left[\langle \alpha_{\uparrow} | \alpha_{\downarrow} \rangle e^{i(\phi - \Delta_\pi\tau)} \right] \right) / 2. \quad (3)$$

We determine $\langle \alpha_{\uparrow} | \alpha_{\downarrow} \rangle$ by observing $P(\uparrow)$ as a function of ϕ and τ . For each value of τ we accumulate the interference fringe pattern as a function of ϕ , and fit it with a sinusoid. To factor out the effect of magnetic field noise, we normalize the observed fringe amplitude by comparison to that obtained in a control experiment, having exactly the same timing but with no \mathcal{W} pulse. The amplitude of the control experiment fringes drop to typically 40% for a 300 μ s spin-echo time.

The observed amplitude A and phase offset ϕ_0 of the fringes are shown as functions of τ for various data sets in figures 2,3. This information enables us to infer the evolution of the system. The analysis is simplified by the fact that critical data exist only where the motion is within the LDR; outside this region the fringe amplitude is close to zero. To fit A we can therefore use a LDR expression [1, 7], modified to take account of the reduction in return time:

$$A(\tau) = e^{-\gamma\tau} \exp(-2D^2 \sin^2(\pi\tau/t_r)). \quad (4)$$

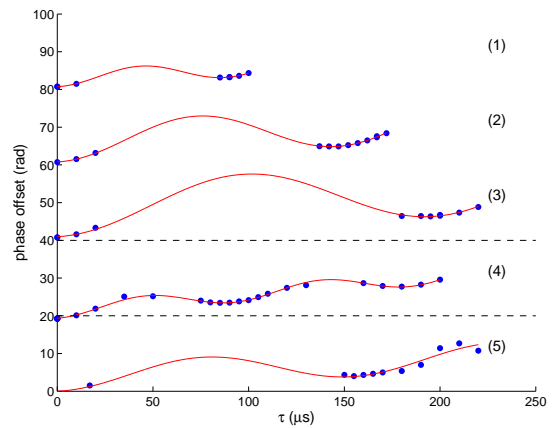


FIG. 3: Observed phase offset of the fringes as a function of τ , successive data sets are offset by 20 radians. The lines are fitted curves using (6), with parameter values given in table 1.

Here γ is mainly a decay caused by decoherence effects[7], but also includes a contribution due to squeezing. The reduction in fringe visibility due to squeezing ranges from less than 1% for data set 1 to approximately 9% for data set 3. The return time t_r constrains the global trajectory, and allows our most direct observations of non-Lamb-Dicke behaviour, in that we find in general t_r is significantly less than $2\pi/\delta$. The parameter D is related to α_0 , the maximum α which would occur for the same force if the motion were entirely within the LDR. We have

$$D = R\alpha_0\sqrt{2\bar{n}_0 + 1} \sin(\Phi_w/2), \quad (5)$$

where the two trajectories are separated by the angle $\Phi_w = |\phi_{\uparrow} - \phi_{\downarrow}|$ and $R = t_r\delta/2\pi$ is the fractional reduction in return time.

The phase is fitted by a similarly modified LDR expression

$$\phi_0(\tau) = (\text{const}) + \Delta_\pi\tau + B^2 \sin^2(\pi\tau/t_r), \quad (6)$$

where $B^2 = R^2\alpha_0^2 \sin(\Phi_w)$.

With the polarization angles in the experiments, $\Phi_w = 1.41(5)\text{rad}$. The amplitude and phase analyses thus each give values of $R\alpha_0$ and t_r . We are then able, using the results of our simulations, to determine R (and hence values for the detuning and α_0), α_{max} and $\Delta\alpha_{\text{max}}$. As a check on the validity of our interpretation we can compare the results obtained for α_0 and $\delta/2\pi$ with those expected on the basis of our knowledge of the laser field. The detuning $\delta/2\pi$ is known to ± 0.5 kHz. Two pieces of information quantify the light intensity: the Rabi flopping rate Ω_c when spin-flip ('carrier') transitions are resonantly driven, and the light shift Δ_π (deduced from (6)) which comes from off-resonant excitation of these same transitions during the \mathcal{W} pulse. The laser polarization is set to be (very close to) linear at the ion for either

set	D	t_r (μs)	γ (ms^{-1})	B	$\Delta_\pi/2\pi$ (kHz)	\bar{n}_0	η	$\Omega_c/2\pi$ (kHz)		$\delta/2\pi$ (kHz)		α_0		α_{\max}	$\Delta\alpha_{\max}$
								a	b	c	d	e	f		
								1	1.45	89	2.0	2.15	4.48		
2	2.27	147	4.1	3.24	4.49	0.07	0.244	139	145	5	5.3	4.5	4.2	3.1	4.0
3	3.12	192	5.6	4.27	4.46	0.07	0.244	139	145	3.5	3.4	6.4	6.8	4.0	5.1
4	1.50	91	3.5	2.03	7.36	0.04	0.199	151	185	10	10.2	2.0	2.3	2.1	2.7
5	1.88	160	4.6	2.72	4.27	0.02	0.245	137	142	-5.5	-5.2	4.0	3.4	2.7	3.5

TABLE I: Experimental parameters and results. Column 1 gives the data set number. The next 5 columns give values extracted directly from the fringe data by curve fitting. The rest of the table gives further raw information and derived quantities. η is known from the trap frequency. Ω_c is obtained by Rabi flopping on the carrier (value a) and from the fitted Δ_π (value b). The detuning δ is set experimentally to within 0.5kHz for a given data set (c) and can be evaluated also (via the TDSE) from the data analysis (d). The same process leads to a value of α_0 (f) which can be compared with that deduced from the parameters of the light field (e). Finally, we infer α_{\max} , the maximum excursion in phase space, and $\Delta\alpha_{\max}$, the maximum distance in phase space between the two spin components, from the TDSE. We estimate b,d,f, α_{\max} and $\Delta\alpha_{\max}$ have 5% accuracy; the consistency check a,c,e combines Rabi flopping, relative power and polarization measurements and is accurate to $\sim 15\%$.

beam acting alone, by nulling any differential light shift observed in Ramsey experiments.

For all the data there is reasonable agreement between observations and predictions. Sets 1–3 were taken on the same day under particularly stable conditions, and have very good overall consistency. The largest α_{\max} and $\Delta\alpha$ (4.0 and 5.1) were obtained with set 3. In particular, we note the large reduction in return time ($R = 0.67$). The results of the numerical solution of the TDSE for this case are shown in figure 1.

The observed coherence is not perfect, owing mainly to magnetic field noise, photon scattering, and heating. The effect of the first of these is small when we use the spin-echo sequence. Let $a \leq 1$ be the predicted overlap of the squeezed states at the return time in a perfect experiment, then $\gamma = \gamma_s + \gamma_m - \ln(a)/t_r$, where γ_s is caused by the laser pulse \mathcal{W} , chiefly by photon scattering, and γ_m quantifies the decoherence of the cat itself, chiefly due to motional effects (electric field noise). We see in sets 1–3 behaviour consistent with the expected $\Delta\alpha^2$ scaling of γ_m [1, 7, 9, 11]. We extracted γ_s from control experiments at large (200 kHz) detuning, where γ_m is small. After adjusting for the laser beam power used in sets 1–3, the observed value $\gamma_s = 1.7(2) \text{ ms}^{-1}$ agreed with the photon scattering rate measured in a separate test by detecting spin-flips. For data set (3) the TDSE gives $a = 0.85$ so we obtain $\gamma_m = 3.0(2) \text{ ms}^{-1}$. This is an average over a changing $\Delta\alpha$: the coherence time $T_2 = 1/2\gamma_m = 170(10) \mu\text{s}$ for this cat state at its maximum excursion.

Numerical simulations showed that the maximum excursion reached in phase space, α_{\max} , is a function of only η and α_0 . For $\alpha_0 > 1$ a third order polynomial fit of the numerical solutions gave

$$\alpha_{\max} \simeq (0.076827x^3 - 0.45539x^2 + 1.1352x - 0.011266)/\eta \quad (7)$$

where $x = \eta\alpha_0$. Also, the fractional change in the time taken for the wavepacket to return to the origin, compared to LDR behaviour, is linear in the fractional change in maximum excursion, i.e.

$$1 - R = \frac{t_0 - t}{t_0} \approx 0.82 \frac{\alpha_0 - \alpha_{\max}}{\alpha_0}. \quad (8)$$

We have studied theoretically the forced motion of a quantum oscillator subject to a moving periodic potential, and experimentally demonstrated large Schrödinger cat-like states of spin and motion of a trapped ion, in which the return time reveals the non-uniform nature of the force, and the inferred motion is such that squeezing is confidently expected to be present though not directly detected. The coherence time is more than an order of magnitude longer than previously reported for this size of cat, due to the low heating rate in our trap. The low heating rate is a result of the comparatively large size of our trap. The coherence time is limited by photon scattering and motional heating. The first of these could be reduced by detuning the Raman laser further from resonance, while the second could be reduced by increasing the trap size or cooling the electrodes to reduce the effect of fluctuating patch potentials on the electrodes. The issues studied here are also relevant to quantum information experiments where forced motion is used to implement 2-qubit quantum logic gates, and high precision is essential[16, 20, 21].

This work was supported by EPSRC (QIP IRC), the Royal Society, the European Union, the National Security Agency (NSA) and Disruptive Technology Office (DTO) (W911NF-05-1-0297).

[1] D. F. Walls and G. J. Milburn, *Quantum Optics* (Springer, Berlin, 1994).

- [2] M. D. LaHaye and et al, *Science* **304**, 74 (2004).
- [3] W. K. Hensinger, D. W. Utami, H.-S. Goan, K. Schwab, C. Monroe, and G. J. Milburn, *Phys. Rev. A* **72**, 041405(R) (2005).
- [4] M. A. Nielsen and I. L. Chuang, *Quantum Computation and Quantum Information* (Cambridge University Press, Cambridge, 2000).
- [5] S. Braunstein and P. van Loock, *Rev. Mod. Phys.* **77**, 513 (2005).
- [6] E. Schrödinger, *Naturwissenschaften* **23**, 807,823,844 (1935), reprinted in English in [22].
- [7] Q. A. Turchette, C. J. Myatt, B. E. King, C. A. Sackett, D. Kielpinski, W. M. Itano, C. Monroe, and D. J. Wineland, *Phys. Rev. A* **62**, 053807 (2000).
- [8] C. Monroe, D. M. Meekhof, B. E. King, and D. J. Wineland, *Science* **272**, 1131 (1996).
- [9] C. J. Myatt, B. E. King, Q. A. Turchette, C. A. Sackett, Kielpinski, W. M. Itano, C. Monroe, and D. J. Wineland, *Nature* **403**, 269 (2000).
- [10] P. C. Haljan, K.-A. Brickman, L. Deslauriers, P. J. Lee, and C. Monroe, *Phys. Rev. Lett.* **94**, 153602 (2005), quant-ph/0411068.
- [11] M. Brune, E. Hagley, J. Dreyer, X. Maître, A. Maali, C. Wunderlich, J. M. Raimond, and S. Haroche, *Phys. Rev. Lett.* **77**, 4887 (1996).
- [12] J. M. Raimond, M. Brune, and S. Haroche, *Rev. Mod. Phys.* **73**, 565 (2001).
- [13] Larger cat states were also created in refs [8, 10, 23], with coherence not observed but likely to be good.
- [14] S. Wallentowitz and W. Vogel, *Phys. Rev. A* **55**, 4438 (1997).
- [15] P. Carruthers and M. M. Nieto, *Am. J. Phys.* **7**, 537 (1965).
- [16] D. Leibfried, B. DeMarco, V. Meyer, D. Lucas, M. Barrett, J. Britton, W. M. Itano, B. Jelenkovic, C. Langer, T. Rosenband, et al., *Nature* **422**, 412 (2003).
- [17] D. M. Lucas, A. Ramos, J. P. Home, M. J. McDonnell, S. Nakayama, J.-P. Stacey, S. C. Webster, D. N. Stacey, and A. M. Steane, *Phys. Rev. A* **69**, 012711 (2004).
- [18] The cooling is by Doppler then Raman sideband cooling; spin state preparation is by optical pumping. \bar{n}_0 is measured by comparing sideband strengths, c.f. F. Diedrich *et al.*, *Phys. Rev. Lett.* **62**, 403 (1989).
- [19] M. J. McDonnell, J.-P. Stacey, S. C. Webster, J. P. Home, A. Ramos, D. M. Lucas, D. N. Stacey, and A. M. Steane, *Phys. Rev. Lett.* **93**, 153601 (2004).
- [20] D. Leibfried, E. Knill, S. Seidelin, J. Britton, R. B. Blakestad, J. Chiaverini, D. B. Hume, W. M. Itano, J. D. Jost, C. Langer, et al., *Nature* **438**, 639 (2005).
- [21] H. Häffner, W. Hänsel, C. F. Roos, J. Benhelm, D. Chek-al-kar, M. Chwalla, T. Körber, U. D. Rapol, M. Riebe, P. O. Schmidt, et al., *Nature* **438**, 643 (2005).
- [22] J. A. Wheeler and W. H. Zurek, *Quantum theory of measurement* (Princeton University Press, Princeton NJ, 1983).
- [23] A. Auffeves, P. Maioli, T. Meunier, S. Gleyzes, G. Nogues, M. Brune, J. M. Raimond, and S. Haroche, *Phys. Rev. Lett.* **91**, 230405 (2003).